Scripta Materialia 48 (2003) 507–512

Synthesis, characterisation and properties of Ni/PSZ and Ni/YSZ nanocomposites

S.T. Aruna *, K.S. Rajam *

Surface Engineering Division, National Aerospace Laboratories, Airport Road, Post Bag No. 1779, Bangalore 560 017, India

Received 3 October 2002; received in revised form 3 October 2002; accepted 8 October 2002

Abstract

Nanocrystalline partially stabilised zirconia (PSZ) and yttria-fully stabilised zirconia (YSZ) powders were prepared by solution combustion process. Nanocrystalline nature of the powders was confirmed by XRD and TEM. Nanocomposite Ni/PSZ and Ni/YSZ films were electrodeposited from a suspension of nanoparticles in nickel sulfamate solution. The strengthening of the nanocomposite due to nanoparticle incorporation was characterised by nanohardness measurements.

Keywords: Solution combustion; XRD; TEM; Metal matrix composite; Nanohardness

1. Introduction

In recent years, increasing efforts are directed towards the synthesis of nanomaterials because of their improved properties when compared to conventional coarse grained polycrystalline materials [1]. Nanomaterials exhibit increased strength/hardness, enhanced diffusivity, improved ductility/toughness, reduced density, reduced elastic modulus, higher electrical resistivity, increased specific heat, superior soft magnetic properties etc. For example, the Vickers hardness for Ni increases from 140 to 650 on decreasing the grain size from 10 μm to 10 nm [2].

Similarly, metal matrix nanocomposites can be formed by the addition of nanometer-sized particles to a host matrix like Ni. The fabrication of nanocomposites provides a method for synthesising materials with properties tailored for specific applications like wear resistant coatings, self-lubricating films, and thermally graded coatings. In the literature certain nanosize materials like ZrO_2, Al_2O_3, TiO_2 have been incorporated in nickel matrix to form nanocomposites [3–6].

The unique mechanical and electronic properties of zirconia (ZrO_2) ceramics have led to their widespread use as structural materials, solid-state electrolytes, and thermal barrier coatings [7]. It exists in three different polymorphs: the low-temperature (room temperature) $P2_1/c$ monoclinic (m) structure, the intermediate-temperature (above 1173 °C) $P4_2/nmc$ tetragonal (t) structure and the high-temperature (above 2370 °C) Fm3m (c) cubic structure and the phase transformation of t-phase

* Corresponding authors. Tel.: +91-80-5086247/250; fax: +91-80-5210113.

E-mail addresses: aruna_reddy@css.cmmacs.ernet.in (S.T. Aruna), rajam@css.cmmacs.ernet.in (K.S. Rajam).

1359-6462/03/$ - see front matter
PII: S1359-6462(02)00498-0

to m-phase is accompanied by significant volume expansion (3–5 vol.%). The addition of several oxides (Y_2O_3, CeO_2, MgO, etc.) can stabilise the high-temperature cubic phase in ZrO_2, so the occurrence of monoclinic ZrO_2 can be repressed [8]. Partially stabilized zirconia (PSZ) has many superior properties such as high melting temperature, low thermal conductivity and high chemical stability and it is well known for its transformation toughening behaviour [9]. On the other hand, yttria-fully stabilised zirconia (YSZ) has a unique combination of mechanical properties such as excellent thermal stability, high fracture toughness, Young's modulus and thermal expansion coefficient close to steel [10]. Since YSZ has reversible expansion–contraction behaviour on thermal cycling without any disruptive phase transitions, YSZ can be a better candidate than PSZ for various applications.

In the literature, as far as our knowledge goes there are no reports on comparative studies of Ni/PSZ and Ni/YSZ nanocomposites. Electro-deposition provides a cost-effective means of producing fully dense nanocrystalline metals, alloys and metal-matrix composites [11]. The present work has the purpose of synthesising nanostructured Ni–zirconia composite layers by electrodeposition of nanosize PSZ and YSZ particles and investigating their mechanical properties.

There are various methods reported in the literature for the preparation of nanosize PSZ and YSZ powders like mechano-chemical milling [12], spray drying of an aqueous slurry of the respective oxides or salts [13], inert-gas condensation [14], plasma technique [15], sol–gel process [16], coprecipitation [17], hydrothermal process [18] and microwave-hydrothermal process [19]. However, most of these techniques are quite involved and require high temperatures (>1000 °C) and long processing time. Solution combustion (SC) process is emerging as a promising technique for the preparation of advanced ceramics, catalysts and nanomaterials [20]. This process is simple, fast, economic, does not require high temperature furnaces and complicated set-ups. It can be used for the preparation of all kinds of oxides. One can also prepare nanosize oxides in a single step by this technique by changing the oxidisers and fuels [21]. In the present work nanosize PSZ and YSZ have been prepared by SC process.

2. Experimental

2.1. Synthesis of nanosize PSZ and YSZ by SC process

Nanosize PSZ was synthesised by SC technique by rapidly heating an aqueous saturated solution containing stoichiometric amounts of zirconium nitrate and glycine mixture. Stoichiometric composition of the redox mixture was calculated based on the total oxidising (O) and reducing (F) valencies of the oxidiser and the fuel keeping the O/F ratio unity [22]. According to the O/F concept, the molar ratio of zirconium nitrate and glycine is 1:1.6. The aqueous solution containing stoichiometric amounts of zirconium nitrate and glycine was rapidly heated on a preheated hot plate (~400 °C). The solution underwent rapid dehydration and foaming, followed by decomposition, generating combustible gases leaving behind a tree like structured white mass which is the desired product. In the literature nanosize ZrO_2 has been prepared by SC process by the use of an extra oxidiser like NH_4NO_3 along with glycine [23]. We assume that NO_2 (brown fumes observed during combustion) was formed along with N_2, H_2O and CO_2 during the combustion reaction of zirconium nitrate and glycine. Theoretically, the complete combustion can be represented as follows:

$$5Zr(NO_3)_{4(aq)} + 8\underset{\text{(glycine)}}{CH_2{-}NH_2{-}COOH_{(aq)}} \rightarrow 5ZrO_{2(s)} + 8CO_{2(g)} + 20H_2O_{(g)} + 15NO_{2(g)} + 13/2N_{2(g)}$$

Similarly, 6 mol% YSZ was prepared by heating an aqueous redox mixture containing zirconium nitrate, yttrium nitrate and glycine in the molar ratio of 1:0.03:2.25. It is noteworthy to mention that the SC process has been scaled up to prepare 50 g of the powder for our experiments in a single batch.

The nanosize PSZ and YSZ powders prepared by SC technique were dispersed in the nickel

sulfamate bath and stirred overnight. The bath loadings of 25, 50 and 80 g/l of PSZ (powder density = 5 g/cm^3) and YSZ particles (powder density = 4 g/cm^3) were used. A nickel sulfamate bath having the following composition was used for plating Ni matrix: 300 g/l nickel sulfamate, 10 g/l nickel chloride, 30 g/l boric acid and 15 ml of 10% sodium lauryl sulfate. The plating bath temperature was held at 45 °C and the pH of the bath was maintained at 4 by the addition of sulfamic acid and basic nickel carbonate. A nickel anode and a brass cathode were used. The polished brass substrate area of 2.5×3.75 cm^2 was degreased with acetone, followed by cathodic cleaning, acid dipping and finally washed with distilled water. The electrodeposition was carried out with Aplab 7253 regulated DC power supply for 3 h using a current density of 1.6 A/dm^2.

The crystallinity and phase identification was performed with Philips X-ray diffractometer using CuK_α radiation. The average particle size was estimated by using the Debye–Scherrer formula, $D = 0.9\lambda/\beta \sin\theta$, where D is the crystallite size, λ is the wavelength of CuK_α radiation, β is the corrected line width at half peak intensity and θ is the diffraction peak angle [24]. Silicon powder with a mean particle diameter of 25 μm was used to measure the instrumental peak broadening in order to correct the value of β. The XRD patterns of the deposited Ni films were recorded in glancing angle geometry using a Rigaku D/max 2200 powder diffractometer with a glancing angle of 3°. The deposits were given a copper backing layer and cut into smaller pieces. Samples were embedded in bakelite and polished to a mirror like finish using standard metallographic techniques to obtain cross sectional samples for hardness and image analysis. Hardness was measured with a Nanohardness Tester, Model-4-114 NHT, CSEM Instruments using a Berkovich diamond indenter with 50 mN load. Young's modulus was determined from the initial unloading portions of the indentation curves. The microstructure and the components of the coating were studied using SEM (Leo 440I) with energy dispersive X-ray analysis attachment. A JEOL-JEM 100SX transmission electron microscope, operating at 120 kV was used to determine the shape and size of the particles.

3. Results and discussion

The XRD patterns of PSZ and YSZ are shown in Fig. 1. From the XRD patterns it is clear that combustion synthesised PSZ and YSZ powders are crystalline. PSZ shows a mixture of t-phase, m-phase and c-phase (Fig. 1(b)) and YSZ shows purely cubic phase (Fig. 1(c)). The X-ray line broadening clearly indicates the nanocrystalline nature of the powders. The average particle size calculated using Debye–Scherrer formula for YSZ and PSZ are 10 and 30 nm respectively. The relative amounts of the t-phase and m-phase in PSZ phase were estimated from the expression

$$V_m = \frac{(I_{m(1\,1\,\bar{1})} + I_{m(1\,1\,1)}) \times 100}{I_{m(1\,1\,\bar{1})} + I_{m(1\,1\,1)} + I_{t(1\,1\,1)}},$$

where I is the intensity of the diffraction peak [25]. The commercial PSZ sample shows 78% monoclinic phase and the rest tetragonal phase (Fig. 1(a)). From the XRD pattern (Fig. 1(b)) it was calculated that the combustion synthesized PSZ powder had 16% m-phase and the remaining t-phase and c-phase. It is interesting to note that by combustion synthesis we could get PSZ with a higher percentage of tetragonal phase (Fig. 1(b)) without the use of a stabilizer. However in the

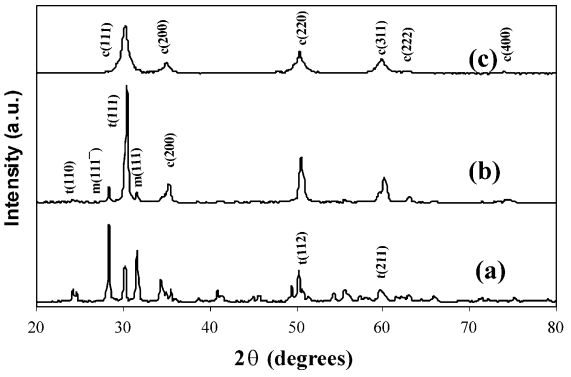

Fig. 1. Powder XRD patterns of (a) commercial PSZ (b) combustion synthesized PSZ and (c) combustion synthesized YSZ.

literature, 3 mol% Y_2O_3 has been used to get PSZ with lower percentage of tetragonal phase and $\geqslant 7$ mol% Y_2O_3 has been used to get YSZ [10]. Thus it is evident that SC is a versatile technique capable of yielding PSZ phase without the use of a stabilizer. From the X-ray line broadening the particle size was calculated for the Ni on Ni/YSZ and Ni/PSZ films with three different particle contents (25, 50 and 80 g/l). The average grain sizes for Ni obtained from the analysis of two different reflection groups (1 1 1) and (2 0 0) are in the nanocrystalline range (25–32 nm) and are not very much affected by the incorporation of nanosize ceramic particles in the Ni matrix. This observation agrees well with that reported in the literature [3]. Peak broadening in plated nanoparticle strengthened nickel films may also be due to the stresses in the specimens. Since the peak broadening did not change much after the particle incorporation we assume that the stresses are negligible. XRD analysis of the Ni/PSZ and Ni/YSZ films indicated a preferred (1 1 1) crystallographic orientation.

The TEM image of PSZ is shown in Fig. 2. From the TEM image we can observe that the particles are *rod-like* to spherical in shape with few agglomerates. Some larger particles present in the TEM (70–150 nm) may correspond to monoclinic phase. The average particle size calculated from TEM (28.5 nm) coincides well with the particle size calculated from X-ray line broadening (30 nm).

The SEM surface morphology of Ni/PSZ (50 g/l) nanostructured composite coating is shown in Fig. 3. It shows a nodular disturbed surface structure and PSZ particles are not clearly visible on the surface because of their smaller dimensions (white particles). The EDX results show a good uniformity of dispersed phase. From the EDX, it is found that wt.% of ZrO_2 codeposited in the nickel matrix varies between 0.30 and 8.4. The wt.% of ZrO_2 codeposited is higher for higher concentrations of PSZ and YSZ in the nickel sulphamate bath. There was good codeposition of YSZ even when the concentration of YSZ was 25 g/l. The optical micrograph of the cross-section of Ni/PSZ reveals uniform particle distribution throughout the nickel matrix with agglomerates (Fig. 4). SEM with EDX was carried out on the cross-section of the samples. The EDX of the rod-shaped appearances corresponds to ZrO_2 ceramic phase. Thus the ceramic particles agglomerate and result in larger particles which may be due to the agglomeration of nanoparticles in the aqueous electrolyte

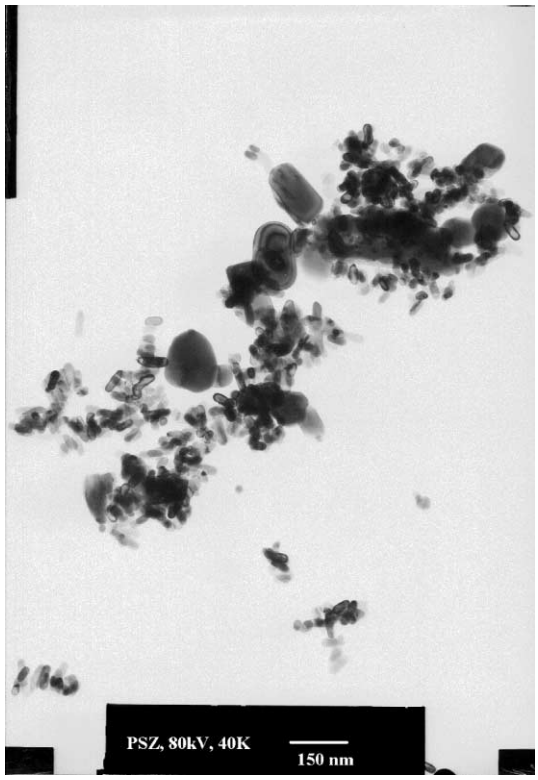

Fig. 2. TEM image of combustion synthesized PSZ powder.

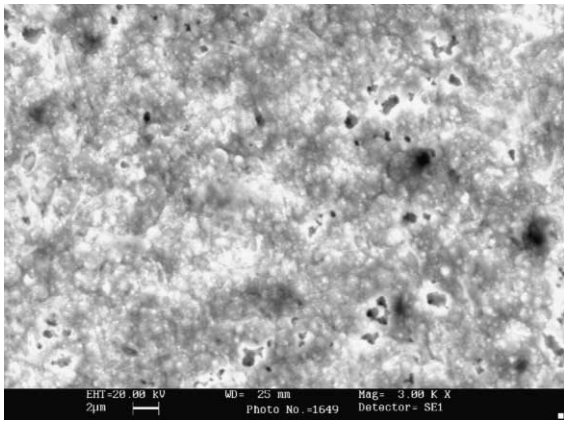

Fig. 3. SEM surface morphology of Ni/PSZ (50 g/l) nanostructured composite coating.

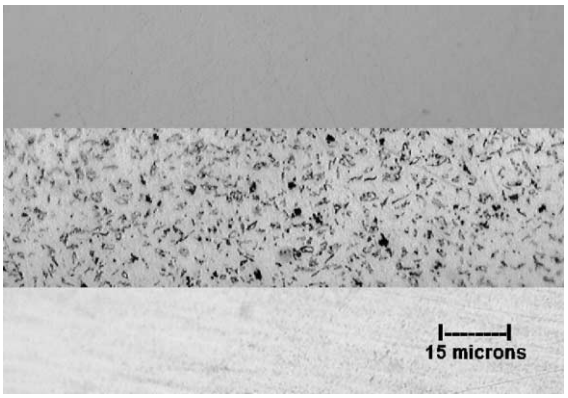

Fig. 4. Optical micrograph of the cross-section of Ni/PSZ (80 g/l) nanocomposite.

[3]. The volume fraction of the particles codeposited was calculated by a microscopic technique. The vol.% of dispersed phase was in the range of 30–35 and 10–15 respectively for 80 g/l YSZ/PSZ and 50 g/l YSZ/PSZ powder dispersion.

The Vickers hardness and Young's modulus values of Ni/YSZ and Ni/PSZ coatings were averaged for five readings and are tabulated in Table 1. From Table 1, the following conclusion can be made: higher the concentration of the particles in the bath, higher will be the incorporation of particles resulting in higher hardness values compared to nickel (~300 VHN at 50 mN). Thus PSZ and YSZ particles have a major hardening effect on the nickel matrix. The increased hardness may be due to the presence of ceramic particles in the metal matrix which may act as obstacles to dislocation movement and grain boundary sliding [3]. Since the matrix grain size of nickel did not change after the incorporation of the ceramic particles and only the hardness values increased, we assume that the increased hardness is due to the nanoparticle incorporation only.

However, YSZ with a particle size of 10 nm in the nickel matrix exhibits higher hardness than PSZ with a particle size of 30 nm in the same nickel matrix. This may be explained as follows: higher the particle number density of the 10 nm particles, more effective will be the pinning of dislocation motion, higher will be the hardness compared to films with 30 nm PSZ [26]. The Vickers hardness of 618 observed for Ni/YSZ (80 g/l) is almost twice

Table 1

Sample	Vickers hardness (50 mN load)	Young's modulus (GPa)
Ni/PSZ (25 g/l)	410	219
Ni/PSZ (50 g/l)	524	243
Ni/PSZ (80 g/l)	559	202
Ni/PSZ (50 g/l)[a]	430	232
Ni/YSZ (25 g/l)	563	228
Ni/YSZ (50 g/l)	584	204
Ni/YSZ (80 g/l)	618	198
Ni/YSZ (50 g/l)[a]	455	214
Ni/YSZ (80 g/l)[a]	458	236

[a] 1.65 g/l sodium lauryl sulfate.

the Vickers hardness of Ni matrix. The values of Vickers hardness obtained in the present study were comparable and relatively higher (for YSZ) than those reported in the literature [3]. When the concentration of the surfactant, sodium lauryl sulfate was increased from 1.5 to 1.65 g/l, the rate of codeposition decreased and consequently the hardness values decreased (Table 1). The decrease in the rate of codeposition may be due to the presence of excess of surfactants on the cathode or due to a strong repulsive force between the surfactant layer on the cathode and the approaching particles [27]. It will be interesting to investigate the role of various cationic surfactants during PSZ and YSZ codeposition and future studies are aimed in that direction.

The Young's modulus decreased with increased nanoparticle incorporation (from ~250 to ~200 GPa) into the Ni matrix. The reduction in the Young's modulus after the particle incorporation may be attributed to the nanocrystalline PSZ and YSZ particles [1].

Future studies are also aimed at (i) the preparation of 10 nm PSZ particles and (ii) to investigate the effect of 10 nm PSZ and YSZ particles on the mechanical properties after their incorporation into the Ni matrix.

4. Conclusions

Nanocrystalline PSZ (30 nm) and YSZ (10 nm) were synthesised by a single step SC route using glycine as fuel and without the use of an extra oxidiser. The process has been scaled up to prepare

50 gm powder in a single batch. The particle size calculated from XRD line broadening (30 nm) coincides well with that obtained from TEM (28.5 nm) for PSZ. The PSZ and YSZ nanoparticles were codeposited in the nickel matrix and the amount of codeposited particles varied between 0.3 and 8.4 wt.% as calculated from EDX. The size of the nickel grains was not affected by the codeposition of nanosize ceramic particles into the nickel matrix. Nanocrystalline Ni/PSZ (80 g/l) and Ni/YSZ (80 g/l) composite coatings produced by codeposition exhibit Vickers hardness of 559 and 618 respectively. The nanocomposites displayed significant hardness enhancements relative to single-phase nickel films. It is concluded that YSZ incorporation into Ni matrix induces higher hardness than PSZ and this may be due to the smaller size of the YSZ particles compared to PSZ particles.

Acknowledgements

The authors are thankful to Tirosh S, Siju, Venkataswamy MA, Anjana and Usha Devi for the TEM, nanohardness, SEM and XRD studies respectively. The authors thank the Director, NAL for giving permission to publish this work.

References

[1] Suryanarayana C. Bull Mater Sci 1994;17:307.
[2] El-Sherik AM, Erb U, Palumbo G, Aust KT. Scripta Metall 1992;27:1185.
[3] Möller A, Hahn H. Nanostruct Mater 1999;12:259.
[4] Müller B, Ferkel H. Z Metallkd 1999;90:868.
[5] Shao I, Vereecken PM, Chien CL, Searson PC, Cammarata RC. J Mater Res 2002;17:1412.
[6] Zhou M, de Tacconi NR, Rajeshwar K. J Electroanal Chem 1997;421:111.
[7] Birkby I, Stevens R. Key Eng Mater 1996;122:527.
[8] Moon J, Choi H, Kim H, Lee C. Surf Coat Technol 2002;155:1.
[9] Lange FF. J Mater Sci 1982;17:225.
[10] Wachtman JB. Mechanical properties of ceramics. New York: Wiley; 1996. p. 173.
[11] Robertson A, Erb U, Palumbo G. Nanostruct Mater 1999;12:1035.
[12] Dodd AC, McCormick PG. J Eur Ceram Soc 2002; 22:1823.
[13] Dodd AC, McCormick PG. Acta Mater 2001;49:4215.
[14] Skandan G. Nanostruct Mater 1995;2:111.
[15] Yi Z, Lee SW, Gao L, Ding CX. J Eur Ceram Soc 2002; 22:347.
[16] Brenier R, Gagnaire A. Thin Solid Films 2001;392:142.
[17] Silva VV, Lameiras FS, Domingues RZ. Ceram Inter 2001; 27:615.
[18] Piticescu RR, Monty C, Taloi D, Motoc A, Axinte S. J Eur Ceram Soc 2001;21:2057.
[19] Potdar HS, Deshpande SB, Deshpande AS, Gokhale SP, Date SK, Khollam YB, Patil AJ. Mater Chem Phys 2002; 74:306.
[20] Patil KC, Aruna ST, Ekambaram S. Curr Opinion Solid State Mater Sci 1997;2:158.
[21] Mimani T. Resonance 2000;5:50.
[22] Kingsley JJ, Patil KC. Mater Lett 1988;6:427.
[23] Mimani T, Patil KC. Mater Phys Mech 2001;4:1.
[24] West AR. Solid State Chemistry and its Applications. Singapore: John Wiley & Sons; 1987. p. 173.
[25] Gravie RC, Nicholson PS. J Am Ceram Soc 1972;55:303.
[26] Shao I, Vereecken PM, Chien CL, Searson PC, Cammarata RC. J Mater Res 2002;17:1412.
[27] Shrestha NK, Miwa I, Saji T. J Electrochem Soc 2001; 148:C106.